Experimental and modelling evidence of splash effects on manure borne Escherichia coli washoff

Claude Mügler, Olivier Ribolzi, Marion Viguier, Jean-Louis Janeau, Emilie Jardé, Keooudone Latsachack, Thierry Henry-Des-Tureaux, Chanthamousone Thammahacksa, Christian Valentin, Oloth Sengtaheuanghoung, et al.

Experimental and modelling evidence of splash effects on manure borne *Escherichia coli* washoff

Claude Mügler[a]*, Olivier Ribolzi[b], Marion Viguier[b], Jean-Louis Janeau[c], Emilie Jardé[d], Keooudone Latsachack[e], Thierry Henry-Des-Tureaux[c], Chanthamousone Thammahacksa[e], Christian Valentin[c], Oloth Sengtaheuanghoung[f], Emma Rochelle-Newall[c]

[a]Laboratoire des Sciences du Climat et de l'Environnement, UMR 8212 CEA-CNRS-UVSQ, Orme des Merisiers, 91191 Gif-sur-Yvette Cedex, France

[b]GET (IRD, Université de Toulouse, CNRS, UPS), 14 avenue Edouard Belin, 31400 Toulouse, France

[c]Sorbonne Université, Univ Paris Est Creteil, IRD, CNRS, INRA, Institute of Ecology and Environmental Sciences (iEES-Paris), F-75005, Paris, France

[d]Univ Rennes, CNRS, Géosciences Rennes, UMR 6118, 35000 Rennes, France

[e]IRD, iEES-Paris, Department of Agricultural Land Management (DALaM), P.O. Box 4199, Ban Nongviengkham, Xaythany District, Vientiane, Lao PDR

[f]Agriculture Land-Use Planning Center (ALUPC), Ministry of Agriculture and Forestry, Vientiane, Lao PDR

*** Corresponding author**: Claude Mügler

E-mail address: claude.mugler@cea.fr

Phone number: 33 (0)1 69 08 93 63

Full postal address: Laboratoire des Sciences du Climat et de l'Environnement, Centre de Saclay, Orme des Merisiers, Bât.714, 91191 Gif-sur-Yvette Cedex, France

Summary: In tropical montane South-East Asia, recent changes in land use have induced increased runoff, soil erosion and in-stream suspended sediment loads. Land use change is also contributing to increased microbial pathogen dissemination and contamination of stream waters. *Escherichia coli* (*E. coli*) is frequently used as an indicator of faecal contamination. Field rain simulations were conducted to examine how *E. coli* is exported from the surface of upland, agricultural soils during runoff events. The objectives were to characterize the loss dynamics of this indicator from agricultural soils contaminated with livestock waste, and to identify the effect of splash on washoff. Experiments were performed on nine 1 m^2 plots, amended or not with pig or poultry manure. Each plot was divided into two 0.5 m^2 sub-plots. One of the two sub-plots was protected with a mosquito net for limiting the raindrop impact effects. Runoff, soil detachment by raindrop impact and its entrainment by runoff, and *E. coli* loads and discharge were measured for each sub-plot. The results show that raindrop impact strongly enhances runoff generation, soil detachment and entrainment and *E. coli* export. When the impact of raindrops was reduced with a mosquito net, total runoff was reduced by more than 50%, soil erosion was on average reduced by 90% and *E. coli* export from the amended soil surface was on average 3 to 8 times lower. A coupled physics-based approach was performed using the Cast3M platform for modelling the time evolutions of runoff, solid particles detachment and transfer, and bacteria transport that were measured for one of the nine plots. After estimation of the saturated hydraulic conductivity, soil erodibility, and attachment rate of bacteria, model outputs were consistent with measured runoff coefficients, suspended sediment and *E. coli* loads. This work therefore underlines the need to maintain adequate vegetation at the soil surface to avoid the erosion and export of soil borne potential pathogens towards downstream aquatic systems.

Keywords: Faecal Indicator Bacteria (FIB); Raindrop impact; Runoff; Physics-based modelling; Tropical agro-ecosystems; Lao PDR

1. Introduction

Globally, there are nearly 1.7 billion cases of diarrhoeal disease every year making it the second leading cause of death in children under five years old (World Health Organisation 2014). A large proportion of this disease load is directly related to the ingestion of water contaminated with microbial pathogens of faecal origin. In urban areas, the majority of faecal contamination is of human origin. However, in rural areas, livestock can also be a significant source of microbial pollution (Gagliardi and Karns 2000; Unc and Goss 2004).

Several bacteria are used as indicators of faecal contamination. However, *Escherichia coli* (*E. coli*) has emerged as one of the most appropriate indicators of microbial contamination of natural waters (Ishii and Sadowsky 2008; Rochelle-Newall et al. 2015). The presence or absence of faecal indicator bacteria (FIB) indicates whether or not faecal contamination is potentially present.

Runoff from manured fields and pastures, as well as direct deposition of animal waste into water are traditionally viewed as important mechanisms of *E. coli* contamination in rural watersheds (Jamieson et al. 2004). The importance of surface runoff during storm events as a mechanism of transport of soil bound *E. coli* was also highlighted by Causse et al. (2015). Ribolzi et al. (2016) showed that the erosion of particles from the soil surface during storm events is a strong source of *E.coli* in rural, montane streams. This is of importance as the majority of enteric bacteria in aquatic systems are associated with sediments and these associations influence their survival and transport characteristics (Jamieson et al. 2005; Muirhead et al. 2006; Wilkinson et al. 1995).

Several authors have demonstrated that overland flow and splash effect (i.e. impact of raindrops on soil surface) are major determinants for soil surface particle detachment and displacement at the plot scale in inter-rill zones (Lacombe et al. 2018; Luk 1979; Quansah 1981; Ziegler et al. 2000). Detached soil particles are then transported downstream by the

splash related droplets and overland flow. Splash and overland flow are interacting processes: kinetic energy dissipation of raindrop impact induces the soil surface sealing, which drastically reduces infiltration (Assouline and Mualem 1997) and favours ponding and overland flow (Mügler et al. 2019); splash results from the compression of the water at the soil surface and thus requires an optimal film thickness for the greatest efficiency which is in the order of 10 mm (Kinnell 1993). Other factors influence the intensity of splash detachment: (i) kinetic energy of drops, which can be increased or reduced depending on the ground cover (Lacombe et al. 2018) or slope angle (Ribolzi et al. 2011); (ii) soil texture, with fine sands being the most sensitive; (iii) soil organic matter content that increases the cohesion of soil particles (Armenise et al. 2018); (iv) soil moisture with low splash detachment when soils are dry and increasingly higher with increasing soil moisture. These processes are often measured on plots of 1 m^2 (Patin et al. 2018).

During the rainy season in tropical humid regions, rainfall intensities are high and the splash effect is known to be a determining factor for the detachment of soil particles (Ziegler et al. 2000). Therefore, given the anticipated links between rain intensity, erosion and the export of soil surface *E. coli* during rain events, it can be hypothesised that the splash effect will have a strong impact on the export of *E. coli* from the soil surface.

Modelling experiments with a physics-based approach is a useful way to understand the physical processes involved. Numerical simulations allow to test different hypotheses on runoff production and the transport of sediments and bacteria. For example, Guber et al. (2009, 2011) coupled the kinematic wave overland flow model KINEROS2 with a convective-dispersive overland transport equation for modelling overland transport of bacteria. The model successfully simulated the release and transport of faecal coliforms on vegetated and bare plots. In a recent paper, we used the physics-based Cast3M code for modelling the impact of raindrops on hydraulic conductivity and overland flow intensity on

steep slopes under high-intensity rainfall (Mügler et al. 2019). The present paper follows on from that work and characterizes the transport of FIB using complementary experimental and modelling approaches.

Rain simulation experiments have been used to examine soil erosion, organic matter export and the impact of various land use practices on soil erosion (Janeau et al. 2014; Le et al. 2020; Tatard et al. 2008). In the present paper, we applied this technique to understand how an indicator of faecal contamination is exported from upland soils used for agricultural activities during a rain event. The objectives of this work were to characterize the loss dynamics of *E. coli* from agricultural soils contaminated with livestock waste and to partition total detachment into the splash and hydraulic components.

2. Materials and methods

2.1. Study area

The rain simulation experiments were conducted in a small mountain Laotian catchment, the Houay Pano catchment (Fig. 1a). This catchment belongs to the Critical Zone Observatory M-Tropics (Multiscale TROPIcal Catchments, https://mtropics.obs-mip.fr). It can be considered as being representative of the montane rural agro-ecosystems of South-East Asia (steep slopes, high rainfall intensities during the rainy season, « slash and burn » agricultural system, contaminated water with microbial pathogens of faecal origin). Shale and schist soil are the most widespread in the catchment and the soil is slightly acidic (Ribolzi et al. 2011). The study area is subject to a tropical climate with heavy rains up to 280 mm h^{-1} (Valentin et al. 2008). Experiments were carried out during the dry season. The agricultural production system is based on a slash and burn technique. Main land use has recently switched from crops and fallow toward teak plantations (Ribolzi et al. 2017). Animal husbandry is now developing. However, animal density remains low with two or three pigs in the lower sections

123 of the catchment and some chickens (~20) in both the lower and upper sections (Rochelle-
124 Newall et al. 2016).
125

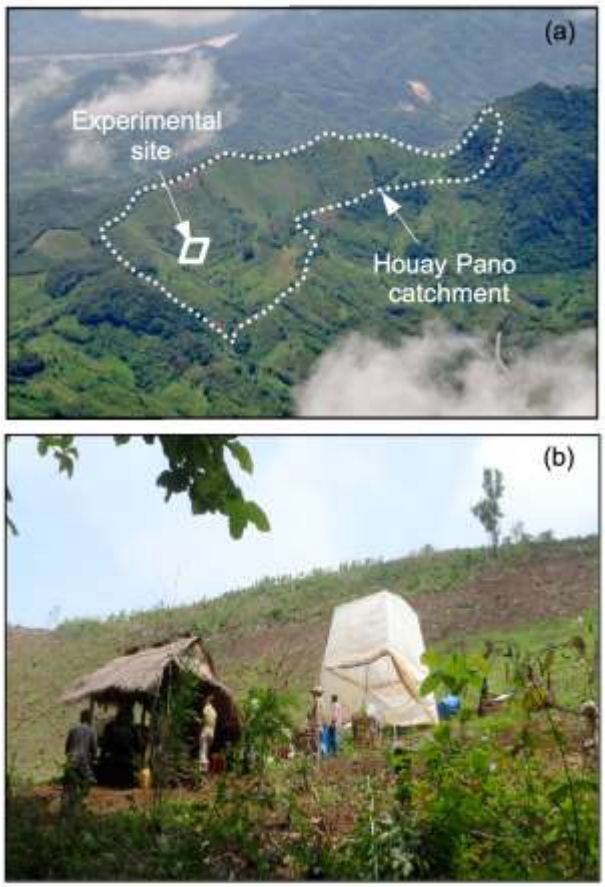

126
127 **Fig. 1** Study site: **(a)** Aerial view of the Houay Pano catchment (white dotted polygon) and
128 location of the experimental site (white rhombus); **(b)** Picture showing an overview of the
129 hillslope and the experimental site with the rainfall simulator tent on the right
130

131 *2.2. Experimental design*

132 Nine 1 m^2 plots were implanted following the method of Janeau et al. (2003) on a steep slope
133 of the upper part of the catchment (Fig. 1b). All the plots had roughly the same steep slope
134 (~48%). The purpose of the study was not to investigate the influence of the slope on the
135 intensity of splash detachment. Indeed, this point has already been studied at Houay Pano by

136 Ribolzi et al. (2011). The soil characteristics (slope, bulk density and texture) are given in
137 Table SI-1 (Online Resource 1). The experimental design was similar to that used by Mügler
138 et al. (2019). Each plot was divided into two sub-plots (1 m downslope × 0.5 m perpendicular
139 to the slope) and one of the sub-plot was covered with a 2-mm grid size wire screen (a
140 mosquito net) (Fig. 2a). The role of the net was to reduce the raindrop impact effects on the
141 soil surface. The nine plots (Fig. 2b) were divided into triplicated treatment groups, denoted
142 A, B, and C: controls with no amendments (Ref A, Ref B and Ref C) or amended with pig
143 manure (Pig A, Pig B, and Pig C) or poultry manure (Chi A, Chi B, and Chi C).
144

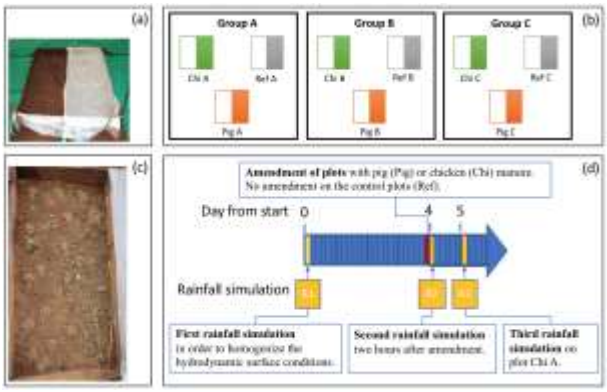

145

146 **Fig. 2** Experimental design: **(a)** image of one 1-m^2 metallic frame divided into two sub-plots
147 without mosquito net (left) and with mosquito net (right); **(b)** Diagram showing the nine plots
148 (pairs of 9 sub-plots without mosquito net shown in white, associated with 9 sub-plots covered
149 with mosquito net shown in colour) divided in triplicated treatment groups (A, B, C): controls
150 with no amendments (Ref A, Ref B, and Ref C) or amended with pig manure (Pig A, Pig B, and
151 Pig C) or poultry manure (Chi A, Chi B, and Chi C); **(c)** Image of one sub-plot partially covered
152 with disconnected small patches of chicken manure ; **(d)** Chronological sequence for the three
153 rainfall simulations (R1, R2 and R3) and time of amendment with pig or chicken manure

154 *2.3. Rainfall simulation*

155 A portable rainfall simulator was used for the three successive rainfall simulations (Fig. 1b).
156 The characteristics of the rainfall simulations were similar to those used and described in
157 Mügler et al. (2019): a constant rainfall intensity ~90 mm h^{-1} during 60 min. The plots were
158 protected with a plastic cover between simulations to prevent the possible modification of the
159 soil surface characteristics and moisture content from natural precipitation. The rain water
160 used for the simulations was pumped from an upland stream adjacent to the plots and samples
161 were collected to determine the background levels of contamination for the rain simulations
162 (Table SI-2, Online Resource 1).

163 The hydrodynamic surface conditions of the nine plots were homogenized by the first rainfall
164 simulation, denoted R1, which was performed without amendment (Fig. 2d). The second
165 rainfall simulation, denoted R2, was carried out on the nine plots 4 days after R1. It was
166 conducted two hours after the input of livestock waste to the Chi and Pig plots (Fig. 2d). No
167 manure was added to the control Ref plots. For the Chi plot of group A, denoted Chi A plot, a
168 third rainfall simulation, denoted R3, was conducted 24 hours after R2 (Fig. 2d).

169 Overland flow from each 0.5 m^2 sub-plot was collected in a large and clean bucket during
170 each rain simulation. Samples of water were collected from each bucket at the end of each
171 rainfall simulation for the determination of total suspended sediment concentration (TSS, g
172 l^{-1}), and *E. coli* numbers (MPN 100 ml^{-1}). These samples represent the average concentration
173 in the runoff water from the 0.5 m^2 sub-plot. During the rainfall simulations R2 and R3 on the
174 Chi A plot, in addition to the average sample, five additional samples were collected over the
175 duration of the simulation to provide an estimation of the time course of *E. coli* export in
176 runoff during two successive rain events. The time course measurements during R3 were only
177 conducted on the Chi A plot. The other plots were destroyed by a very strong natural rainfall
178 event before third series of rain simulations could be completed. As a consequence of the

179 complexity of running this type of experiment in a tropical, upland rural terrain, the rainfall
180 simulations were performed on consecutive days (Fig. 2d). However, care was taken to ensure
181 that the interval of time between simulations was the same throughout the experiment.

182 *2.4. Manure treatments*

183 Pig and chicken manure was collected from six properties in the village of Ban Lak Sip. The
184 manure from each animal type was pooled and mixed. For each 0.5 m^2 sub-plot, 84 g of pig
185 manure or 62 g of chicken waste were mixed with 250 ml of water used for rainfall
186 simulation. These amounts were selected in order to compensate for the higher anticipated
187 *E. coli* loading in chicken manure (Rosebury 1962). Table 1 gives the *E. coli* loads of the
188 manure applied to the plots before the second rainfall simulation, R2. Amended plots were
189 only partially covered by disconnected small patches of manure (Fig. 2c).
190

191 **Table 1:** Most probable number (MPN) of *E. coli* with the associated uncertainty for the soil of
192 the study area and the collected pig (Pig) and poultry (Chi) faeces (wet-weight).

	Measured E. coli (MPN g^{-1})	Error (-)	Error (+)
Soil	5133	1027	12133
Chicken	1.80×10^9	1.02×10^9	2.80×10^9
Pig	0.27×10^9	0.17×10^9	0.43×10^9

193
194

195 *2.5. Determination of TSS and E. coli*

196 The concentration of Total Suspended Sediments (TSS) was measured in each 330 ml sample
197 after filtration on 0.45 μm porosity cellulose acetate pre-weighted filters (Sartorius) and
198 evaporation at 105 °C for 48 h.

E. coli was quantified by standardised microplate method (ISO 8308-3, MUGEC; BioKar®). This method, which has been used with success in this watershed (Boithias et al. 2016; Causse et al. 2015; Ribolzi et al. 2016), is briefly described below. 200 µl of sample were inoculated into each well of the 96-well plate. Six serial dilutions from 1/20 to 1/200000 were used and one plate was used per sample, giving 16 wells per dilution. The limit of detection is low: 15 MPN 100 ml^{-1}. Samples were treated within four hours of collection and were incubated at 44°C for 48 hours. *E. coli* was determined from the number of positive wells using a statistical Poisson distribution (MPN calculator, Build 22 by Mike Curiale).

2.6. Flow, erosion and bacteria transport modelling

The coupling of surface and subsurface flows was performed within a Darcy multidomain approach (Weill et al. 2009). In this approach, flow in the runoff layer, in the unsaturated zone, and in the saturated zone are modelled with a diffusive wave approximation of the Saint-Venant equations, the Darcy equation, and the Richards equation, respectively. The characteristic of the Darcy multidomain approach is to write all these equations in the same way in the whole domain as a single Richards diffusion type equation that describes both surface and subsurface flows. A fuller description of the method is provided in the Supplementary Methods section (Online Resource 1). In the present paper, as validated in Mügler et al. (2019), the saturated hydraulic conductivity K_s was assumed constant in space at the 1-m^2 plot scale but was assumed to decrease with time during the rainfall event due to seal formation according to the following exponential function:

$$K_s(t) = K_\infty + (K_0 - K_\infty)e^{-(Rt/\tau_1)} \quad (1)$$

where R is the rainfall rate [LT^{-1}], τ_1, a dimensioning parameter [L], and K_0 and K_∞, the initial and final hydraulic conductivities [LT^{-1}], respectively (Assouline 2004; Mügler et al. 2019; Ribolzi et al. 2011; Silburn and Connolly 1995).

223 Erosion by soil detachment and entrainment in the runoff layer was modelled with the following
224 sediment mass balance equation

225 $$\frac{\partial hc}{\partial t} + \frac{\partial qc}{\partial x} = e(x,t) \quad (2)$$

226 where c is the depth-averaged sediment concentration [L^3 of sediment /L^3 of water], h is the
227 water depth in the runoff layer [L], and $q=h \times u$ is the water flux [L^2T^{-1}], with u, the runoff
228 velocity. The source term e [LT^{-1}] is usually divided into two contributions: the rate of particle
229 detachment by raindrop impact (hereinafter called splash erosion e_s), and the net rate of particle
230 detachment by flow (hereinafter called hydraulic erosion e_h). At small scale, the dominant
231 erosion mechanism is splash (Kinnell 2005). As a consequence, at the 1-m^2 plot scale, we
232 neglected the hydraulic erosion e_h, and only modelled the splash erosion e_s. Splash erosion is
233 modelled in the same way as in the KINEROS code (Woolhiser et al. 1990)

234 $$e_s(x,t) = c_f(t) \times k(h) \times (R - I)^2 \quad (3)$$

235 where R and I are the rainfall rate and the infiltration rate in the soil [LT^{-1}], respectively. For
236 modelling surface crusting during the rainfall event, we made the choice to model the soil
237 erodibility $c_f(t)$ [$L^{-1}T$] in the same way as we modelled the saturated hydraulic conductivity
238 $K_s(t)$ (Eq. (1))

239 $$c_f(t) = c_\infty + (c_0 - c_\infty)e^{-(Rt/\tau_2)} \quad (4)$$

240 where τ_2 is a dimensioning parameter [L], and c_0 and c_∞ are the initial and final soil
241 erodibilities [$L^{-1}T$], respectively.
242 The function $k(h)$ in Eq. (3) models the decrease of splash erosion rate as surface water depth
243 increases according to the following formulation

244 $$k(h) = e^{-c_h \times h} \quad (5)$$

245 where c_h is the damping coefficient [L^{-1}], which is estimated according to Woolhiser et al.
246 (1990) as follows

$$c_h = 2/d_r \quad (6)$$

where d_r is the raindrop diameter.

Transport of bacteria in the runoff layer was modelled with the following mass balance equation (Guber et al. 2011)

$$\frac{\partial hC_b}{\partial t} + \frac{\partial qC_b}{\partial x} = \frac{\partial}{\partial x}\left(a_L q \frac{\partial C_b}{\partial x}\right) - \frac{\partial S_m}{\partial t} - d\left(k_a C_b - k_d \rho S_s\right) - \left(1 - k_s\right) I C_b + R C_{ir} \quad (7)$$

where C_b, S_m, S_s, and C_{ir} are the cell concentrations in the runoff layer, in the manure applied to the soil surface, in the solid phase of the soil mixing zone, and in the rainfall water, respectively. The mixing zone is the soil surface layer that actively interacts with runoff. Its depth and the soil bulk density in this zone are denoted d and ρ, respectively. The parameters a_L, k_a, k_d, and k_s are the dispersivity [L], the attachment and detachment rates of bacteria at the solid phase [T^{-1}], and the straining coefficient that models the filter due to vegetation, respectively.

The mass conservation of bacteria in the soil mixing zone was given by

$$d\rho \frac{\partial S_s}{\partial t} = d\left(k_a C_b - k_d \rho S_s\right) + k_f \left(1 - k_s\right) I C_b \quad (8)$$

where k_f denotes the fraction of infiltrated cells that are filtered out within the soil-mixing zone. However, Martinez et al. (2014) concluded after a global sensitivity analysis that this parameter was not relevant. Furthermore, the best calibrations of simulations of transport of bacteria performed by Guber et al. (2009, 2011) were obtained with $k_s \sim 1$, showing that the main bacteria exchange between runoff and soil is attachment of bacteria at the solid phase. As a consequence, we took both k_f and k_s equal to one.

The irreversible release of bacteria from the surface applied manure was modelled according to Guber et al. (2011) as follows

$$\frac{\partial S_m}{\partial t} = -C_0 h_m \alpha_m \left(1 + \alpha_m \beta_m t\right)^{-(1+1/\beta_m)} \quad (9)$$

where C_0 is the initial cell concentration in the applied manure [cell L^{-3}], h_m is the thickness of the applied manure, and α_m and β_m are two parameters that characterize the shape of the release curve.

All equations were solved with the numerical code Cast3M. More information about the numerical method and its validation can be found in (Kollet et al. 2017; Mügler et al. 2011; Mügler et al. 2019; Weill et al. 2009). The bacteria transport module was validated with experimental data already published (Guber et al. 2009). Results are described in the Supplementary Methods section (Online Resource 1).

3. Results

3.1. Runoff and erosion

In general, runoff increased from the first simulation (R1) to the second simulation (R2) in all of the plots, regardless of amendment or whether or not netting was present. The average and the standard deviation of the runoff volume from the nine sub-plots where the splash effect was present (those without the netting) was equal to 43 (±12) mm during R1 and increased to 52 (±13) mm during R2 (Fig.3a, left side). In the sub-plots where the splash effect was reduced (those with netting), this average runoff volume increased from 12 (±2) mm to 25 (±6) mm (Fig.3a, right side). The pattern was less clear for soil detachment, although there was for most cases a slight tendency towards decreased soil detachment in R2. Average soil detachment and entrainment in the nine sub-plots where the splash effect was present was equal to 62 (±38) g m^{-2} during R1 and decreased to 54 (±34.0) g m^{-2} during R2 (Fig.3b, left side). In the sub-plots where the splash effect was reduced, this average soil erosion was very low both during R1 (4 (±4) g m^{-2}) and R2 (6 (±5) g m^{-2}) (Fig.3b, right side).

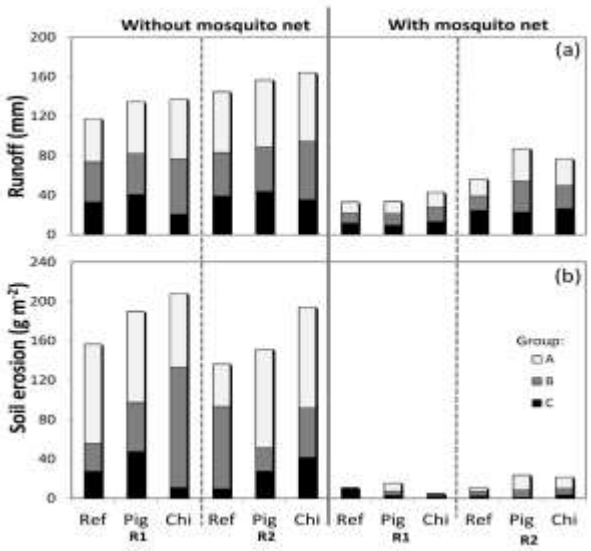

Fig. 3 Bar plots showing cumulated **(a)** runoff depth and **(b)** soil erosion from the eighteen $0.5m^2$ sub-plots (i.e. nine without plus nine with mosquito net) divided into triplicated treatment groups (A, B, C). Controls with no amendments (Ref) or amended with pig manure (Pig) or poultry manure (Chi). Measurements were conducted during the first rainfall simulation (R1, before manure application) and the second rainfall simulation (R2, after manure application)

Large differences in runoff volume and soil erosion were observed between the sub-plots with and without mosquito netting (Fig. 3). This pattern of higher runoff in the splash sub-plots was common to all treatments and all rainfall simulations, regardless of whether manure was added or not. The average runoff volume was ~4 and ~2 times higher in the nine sub-plots where the splash effect was present than in the nine sub-plots where the splash effect was reduced during the first (R1) and second rainfall simulation (R2), respectively. Similarly, average soil erosion on the nine sub-plots where the splash effect was present was nearly one order of magnitude higher than in the sub-plots where the splash effect was reduced after both R1 and R2.

309 *3.2. Escherichia coli load and dynamics*

310 The chicken faeces used contained more than six times more *E. coli* than pig faeces (Table 1).
311 The average concentrations of *E. coli* in runoff collected in the sample bucket at the end of R2
312 were four orders of magnitude higher in the plots that were amended with manure (Fig. 4).
313

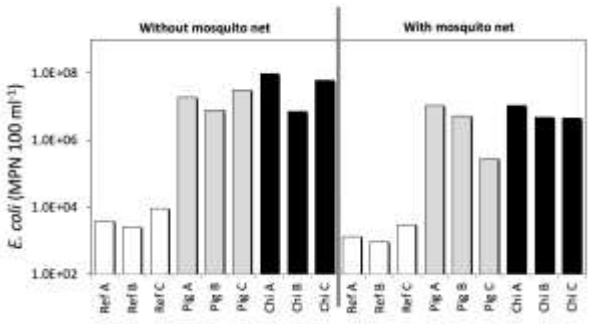

314

315 **Fig. 4** *E. coli* concentration in runoff water from both sub-plots without mosquito net (left
316 side, with splash effect) and with mosquito net (right side, with limited splash effect) for the
317 triplicated plots Ref, Pig, and Chi for rainfall simulation R2
318

319 The average concentrations of *E. coli* in runoff from the Ref plots were 5.2 x 10^3 (± 3.5 x 10^3)
320 and 1.7 x 10^3 (± 1.1 x 10^3) MPN 100 ml^{-1} for the splash and non-splash plots, respectively.
321 These values are of the same order of magnitude as the *E. coli* concentrations measured in the
322 stream water used for the rain during these Ref rainfall simulations (Table SI-2, Online
323 Resource 1). *E. coli* concentrations increased to 1.9 x 10^7 (±1.1 x 10^7) and 5.5 x 10^6 (±5.4 x
324 10^6) MPN 100 ml^{-1} for the Pig splash and non-splash plots and 5.5 x 10^7 (± 4.6 x 10^7) and 6.7
325 x 10^6 (±3.7 x 10^6) MPN 100 ml^{-1} for the Chi splash and non-splash, respectively. Comparing
326 the splash and non-splash plots, the concentrations of *E. coli* were 3, 3.5 and 8 times lower for
327 Ref, Pig and Chi, respectively.
328 The concentration of *E. coli* in runoff was significantly correlated with suspended sediment
329 concentrations in the splash sub-plots ($r^2 = 0.68$; $p < 0.05$) for R2 and R3 on the Chi A sub-

330 plots. No significant correlation was observed for the non-splash sub-plots (Fig. SI-2, Online
331 Resource 1).

332 *3.3. Surface runoff modelling*

333 The modelling approach was used to simulate the time course experiment performed on the two
334 Chi A sub-plots during two successive rainfall simulations R2 and R3. Figures 5a-b display both
335 experiment and model overland flow coefficients. This coefficient is equal to the ratio between
336 the overland flow rate and the rainfall rate. Model outputs were obtained with the parameter
337 values listed in Table SI-3 in the Supplementary Methods section (Online Resource 1). These
338 values are the same as those already used and discussed in Mügler et al. (2019). Only the
339 saturated hydraulic conductivity was estimated. The characteristics of the time evolutions $K_s(t)$
340 used for modelling the runoff (cf. Eq. (1)) are given in Table 2. Runoff in the sub-plot without a
341 mosquito net (splash plots) was correctly modelled with a fast decreasing $K_s(t)$, with the same
342 τ_1 value for the two successive rainfalls ($\tau_1 = 21.4$ mm), and with values of K_0 and K_∞ that
343 were higher in the modelling of R2 than in R3. On the contrary, runoff in the sub-plot with a
344 mosquito net was correctly modelled with a slow decreasing $K_s(t)$, with a nearly one order of
345 magnitude higher value for τ_1 ($\tau_1 = 187.5$ mm). Here again, the value of K_0 decreased from R2
346 to R3. However, the value for K_∞ was the same for both rainfalls. The smaller values of K_0 in
347 the modelling of runoff on the sub-plot without a mosquito net are probably due to the raindrop
348 impact during the preliminary rainfall (before the manure application).
349

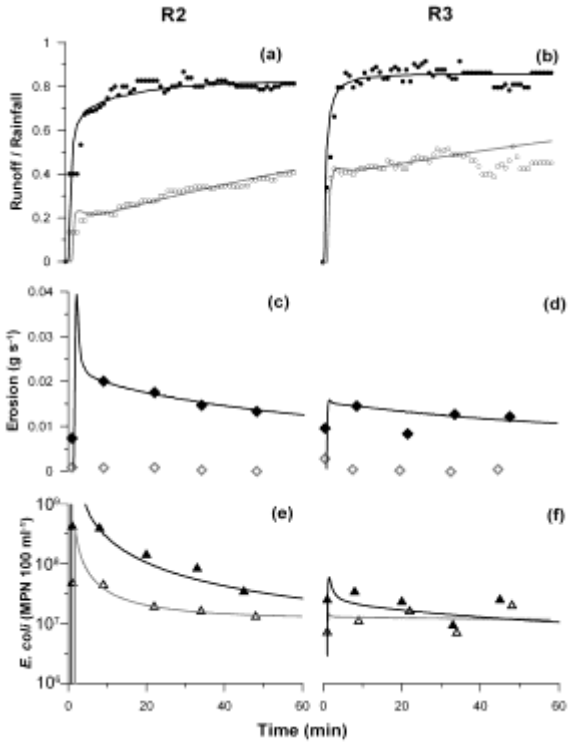

Fig. 5 Evolution over time on plot Chi A of the runoff coefficient (Runoff/Rainfall) obtained during R2 **(a)** and R3 **(b)**; the sediment outputs obtained during R2 **(c)** and R3 **(d)**; *E. coli* concentrations obtained during R2 **(e)** and R3 **(f).** In each figure, empty and filled symbols correspond to the experimental results for the sub-plots with and without a mosquito net, respectively. Solid lines correspond to the modelled evolutions with mosquito net (grey) and without mosquito net (black)

Table 2: Estimated parameter values for the time evolution of saturated hydraulic conductivity $K_s(t)$ given by Eq. (1) and obtained for the two Chi A sub-plot experiments, with and without raindrop impact, and for two successive rainfall simulations R2 and R3.

Sub-plot	Rainfall simulation	τ_1 (mm)	K_0 (mm h^{-1})	K_∞ (mm h^{-1})
without a mosquito net	R2	21.4	40	18
without a mosquito net	R3	21.4	20	14
with a mosquito net	R2	187.5	84	16
with a mosquito net	R3	187.5	62	16

360

361 *3.4. Erosion modelling*

362 Figures 5c-d show the evolutions over time of both measured and modelled sediment outputs
363 during R2 and R3 on the Chi A sub-plots. The comparison of sediment outputs with or without a
364 mosquito net clearly shows the large effect of raindrop impact on erosion. Sediment outputs
365 from the sub-plot for which the surface soil is protected from raindrop impact by a mosquito net
366 are negligible indicating that splash erosion is negligible when the raindrop impact is reduced. It
367 also supports the assumption that hydraulic erosion is negligible at the 1-m^2 plot scale. As a
368 consequence, only the experiment with the raindrop impact was modelled with Eqs (2)-(6).

369 For a ~90 mm h^{-1} rainfall rate, the raindrop diameter d_r is approximately equal to 1.34 mm
370 (Mügler et al. 2019). Thus, according to Eq. (6), the damping coefficient c_h ~1493 m^{-1}. Table 3
371 lists the values of the other erosion parameters which were estimated from the experimental
372 time evolutions of the sediment outputs plotted in Figs. 5c-d.

373

374 **Table 3**: Estimated parameter values for the time evolution of soil erodibility $c_f(t)$ given by
375 Eq. (4) and obtained for the sub-plot experiment without a mosquito net, and for two successive
376 rainfall simulations R2 and R3.

Sub-plot	Rainfall simulation	τ_2 (mm)	c_0 (s m^{-1})	c_∞ (s m^{-1})
without a mosquito net	R2	75	21	8
without a mosquito net	R3	75	15	8

377

378 After rainfall, crusts covered nearly 98% of the surface of the unprotected sub-plot and 77% of
379 the surface of the protected sub-plot, which was already crusted prior to the experiments. The

most impervious crusts, namely gravel and erosion crusts, developed only on the unprotected sub-plot, covering 1.5% and 6% of the surface, respectively (Mügler et al. 2019).

3.5. E. coli transport modelling

Figures 5e-f show *E. coli* concentrations in runoff water at the outlet of the Chi A sub-plots during R2 and R3. The numbers of exported *E. coli* are clearly higher on the sub-plots whose soil surface is not protected from raindrop impact. Table 4 lists the values of two parameter sets, denoted as Model 1 and Model 2 that were used for the bacteria transport modelling. Most of the parameter values in the two sets are the same because they were either measured or determined from the literature. As mentioned in Table 1, the MPN of *E. coli* in poultry faeces was equal to 1.8×10^{9} MPN g^{-1}, and 62 g of chicken waste were applied to each sub-plot. As a consequence, we took $C_0h_m = 2.23\times10^{11}$ MPN m^{-2}. Furthermore, as the *E. coli* concentration in the stream water used for the rain during each rainfall simulation was several orders of magnitude lower than C_0h_m (Table SI-2 in Online Resource 1), the last term in Eq. (7) was removed ($C_{ir} = 0$).

Parameters that characterize the shape of the release curve according to Eq. (9) were estimated from the fit of experimental release of faecal coliform from manure on plots (Guber et al. 2006). Guber et al. (2006) showed that the value of α_m in Eq. (9) was linearly related to the rainfall rate R (cm h^{-1}) according to the following relationship: $\alpha_m = 0.036 + 0.86\times R$. For bare clay loam plots and irrigation rates ~ 6 cm h^{-1}, they found that experimental evolutions were correctly fitted with $\beta_m = 8$. As a consequence, we took these values (see Table 4).

403 **Table 4:** Parameter values for the bacteria transport modelling.

Parameters	Symbol	Unit	Model 1	Model 2
Initial cell concentration	$C_0 h_m$	MPN m^{-2}	2.23×10^{11}	same value
Cell concentration in the rainfall	C_{ir}	MPN m^{-2}	0	same value
Shape of the release curve	α_m	h^{-1}	$0.036 + 0.86\times R$ (R in cm h^{-1})	same value
	β_m	-	8	same value
Thickness of the active soil layer	D	M	0.01	same value
Dispersivity	a_L	M	0	same value
Partitioning coefficient	K_d	ml g^{-1}	54	same value
Attachment rate	k_a	s^{-1}	0	0.015 (estimated)
Detachment rate	$k_d = k_a/((\rho/\theta_s)\times K_d)$	s^{-1}	0	1.4×10^{-4}

404

405 The thickness of the soil mixing zone, d, was set at 1 cm (Cho et al. 2016; Guber et al. 2011).
406 Dispersivity was neglected at the 1-m^2 plot scale ($a_L = 0$). The partitioning coefficient K_d, which
407 is defined as $k_a/((\rho/\theta_{sat})\times k_d)$, was assumed to be related to the clay content in the soil as follows
408 (Pachepsky et al. 2006)

409 $$K_d = A \times (CLAY)^B \quad (10)$$

410 where CLAY is the clay percentage in soil, and parameters $A=10^{-1.6 \pm 0.9}$, and $B=1.98 \pm 0.7$. This
411 relation gave us K_d = 54 ml g^{-1}. Finally, the only difference between Model 1 and Model 2 was
412 that the interaction between the mixing zone and the runoff was neglected in Model 1 ($k_a = k_d =$
413 0), although the attachment and detachment of bacteria to the solid phase, and the infiltration of
414 bacteria in the soil were taken into account in Model 2 ($k_a \neq 0$ and $k_d \neq 0$). Hence, in Model 1,

all parameters were estimated *a priori*. None were calibrated. On the contrary, in Model 2, the attachment rate of bacteria at the solid phase, k_a, had to be estimated from experimental results. Thus, the detachment rate of bacteria, k_d, was calculated as $k_d=k_a/((\rho/\theta_{sat})\times K_d)$.

In Figs. 5e-f, the black solid lines correspond to the evolutions over time of *E. coli* export obtained during the two successive simulated rainfalls with Model 1. Except at the beginning of runoff when the simulated concentration is very high because the runoff layer is extremely thin, the numerical results are in good agreement with the experimental results on the sub-plot with raindrop impact, both during the first and the second rainfall (filled triangles in Figs. 5e-f). This result was obtained without calibration. In contrast, the exported bacteria concentrations measured at the outlet of the sub-plot whose surface soil was protected from raindrop impact (empty triangles in Figs. 5e-f) were correctly simulated with Model 2 (grey solid lines in Figs. 5e-f) after estimation of the attachment rate k_a to the value 0.015 s^{-1}.

4. Discussion

Runoff from manured fields and pastures is known to be an important mechanism by which organisms of faecal origin are transferred to streams highlighting the dominance of diffuse sources of contamination over point sources in rural watersheds (Collins et al. 2005). This is particularly the case in rural areas of developing countries where solid and liquid waste from humans and other animals is released into the environment without treatment. We used field rain simulations and modelling to examine how *E. coli* are exported from the surface of upland, agricultural soils during runoff events.

4.1. Effect of raindrop impact on overland flow and soil detachment and entrainment

When the impact of raindrops was reduced, total runoff was on average reduced by 70% during the first rainfall simulation and by 50% during the second one (Fig. 3a). The purpose of the modelling approach was not to perform a precise calibration of all parameters but rather

439 to investigate the behaviour of some of them. Runoff was correctly modelled with a saturated
440 hydraulic conductivity decreasing with time during the rainfall event (Figs. 5a-b). This
441 decreasing conductivity of the soil was faster for the sub-plot without a mosquito net than for
442 the protected sub-plot. This behaviour can be attributed to the formation of more structural
443 crusts on the unprotected soil surface subject to the high kinetic energy raindrop impacts
444 (Mügler et al. 2019).
445 As shown by many previous studies (Wei et al. 2007; Lacombe et al. 2018), the intensity of
446 rain and soil detachability are directly related. As Ziegler et al. (2000) observed, splash effects
447 dominate over hydrologic processes in soil detachment. Figures 3 and 5 show that rain splash
448 not only enhances runoff generation but also greatly contributes to soil detachment and
449 entrainment. Such a high value of soil detachment rate has already been noticed on bare soils.
450 For example, Patin et al. (2018) obtained in the same catchment a mean soil loss per rainfall
451 event of 154±53 g m^{-2} on bare soils. This rate dropped to 2 g m^{-2} when the soil was left
452 fallow. In our experiments, the mosquito net, which reduces the splash erosion by 90%, plays
453 the same role as a low vegetation cover.

454 *4.2. Effect of raindrop impact on bacteria export*

455 Figures 4 and 5e-f show that rain splash also has a strong impact on the export of *E. coli* from
456 the soil surface. The modelling approach used in the work presented here allows the
457 determination of the main processes involved in the transport of bacteria. In this approach
458 (Eqs. 7-9), bacteria are assumed to be released from the surface applied manure into the
459 runoff water. Then, they can interact or not with the soil surface layer. In this zone, called the
460 “soil mixing zone”, bacteria can attach or detach from the solid phase. In the sub-plot where
461 the raindrop impact was not reduced (without mosquito net), the high experimental bacteria
462 export was correctly modelled without any exchange of bacteria between runoff and mixing
463 zone. This behaviour is in agreement with experimental and numerical results of Guber et al.

464 (2009) that we used to validate our modelling approach. Guber et al. (2009) calibrated the
465 mass exchange rate between the runoff and the mixing zone to zero for modelling the export
466 of bacteria from bare plots subject to high rainfall intensities ($58 < R < 73$ mm h^{-1}).
467 In contrast, less bacteria were exported from the sub-plot where raindrop impact was reduced
468 (with mosquito net). In this case, a part of the bacteria that were released from the manure into
469 the runoff water interacted with the soil surface layer. This lower bacteria export from a
470 protected sub-plot was correctly modelled by taking into account the exchange of bacteria
471 between the overland flow and the soil by attachment and detachment. This behaviour is in
472 agreement with model results of Guber et al. (2011). Indeed, from the calibration of field-
473 scale experiments subjected to rainfall rates lower than 14 mm h^{-1}, Guber et al. (2011)
474 concluded that adsorption and desorption of bacteria released from dairy bovine manure were
475 not negligible. The k_a/k_d ratio that they obtained from calibration (k_a/k_d~122) is comparable to
476 the value that we obtained (k_a/k_d~107).

477 *4.3. Effect of successive rainfalls*

478 As can be seen in Fig. 3a, for each plot, runoff depth increases during successive rainfalls.
479 This increase was correctly modelled by a decrease of the initial hydraulic conductivity K_0
480 from one rainfall to the next (Table 2 and Figs 5a-b). Effect of successive rainfalls on soil
481 detachment is more contrasted. On one hand, there was a tendency towards decreased soil
482 detachment and entrainment from the sub-plots without mosquito net during successive
483 rainfalls (Fig. 3b). On the other hand, when the impact of raindrops was reduced, soil
484 detachment and entrainment was negligible on the non-amended subplots during both the R1
485 and R2 rainfalls. It only slightly increased during R2 on the amended Pig A and Chi A sub-
486 plots perhaps because of the entrainment of some manure by runoff. It is also potentially due
487 to an indirect effect linked to the evolution of the deposit between the two rainfall simulations
488 (e.g. solar radiation, biological activity) that would have made the deposit easier to mobilize.

When the impact of raindrop was reduced by the mosquito net, the concentration of *E. coli* in runoff decreased mainly during the first 20 min of rainfall R2 (Fig. 5e). Thereafter, the concentration decreased only very slightly during the following rainfall R3 (Fig. 5f). When the sub-plots were not protected with a mosquito net, concentrations of *E. coli* in runoff were ten times higher and decreased during the successive rainfalls R2 and R3 (Figs 5e-f). Although the data from the rainfall R3 should be viewed with caution given that only one experiment was possible, the data point towards a decreasing dynamic over successive rainfalls. This decline of the peak bacteria release between the once-wet faecal deposit and subsequent rainfall events has long been observed (e.g. Kress and Gifford 1984). It has been attributed to the leaching effect of the first rainfall on bacteria in the faecal deposit.

5. Conclusion

Rainfall simulation experiments at the plot scale carried out with or without raindrop impact on bare or amended soils led to the following conclusions:

- Runoff production, soil detachment and entrainment and *E. coli* export are strongly enhanced by raindrop impact. When the impact of raindrops was reduced with a mosquito net, soil erosion was on average reduced by 90% and *E. coli* export from the amended soil surface was on average 3 to 8 times lower. These results underline the strong impact of the splash effect on the export of *E. coli* from the soil surface.
- The temporal evolution of runoff, soil and *E. coli* exports during two successive rainfall simulations were correctly modelled with a physics-based approach with a soil hydraulic conductivity and a soil erodibility that exponentially decreased over time of exposure to rainfall. These decreasing parameters model the splash effect on the soil surface properties.
- Both experimental and modelling approaches showed the leaching effect of the first rainfall on bacteria in the faecal deposit.

514 • When the impact of raindrops was reduced, the lower bacteria export from the protected
515 soil was correctly modelled by taking into account the exchange of bacteria between the
516 overland flow and the soil by attachment and detachment.
517
518 These results highlight the strong mobilization and transport of faecal indicator bacteria from
519 steep slopes under high intensity rainfall such as usually occur in rural Southeast Asia. The
520 links between land cover, or vegetation and soil erosion have been previously identified (i.e.
521 Lacombe et al. 2018) and recent work demonstrated the importance of vegetation cover in
522 reducing the export of soil microbial communities from soils (Le et al. 2020). The work
523 presented here builds on this work and shows that by reducing the splash effect, through low
524 cover, such as surface vegetation, can significantly reduce microbial pathogen dissemination
525 and, by extension, the contamination of stream waters. This is particularly important in areas
526 where access the adequate sanitation is limited or non-existent and where untreated surface
527 water is used for domestic requirements.
528
529

Declarations

Ethics approval and consent to participate

Not applicable

Consent for publication

Not applicable

Availability of data and materials

The datasets used and analysed during the current study are available from the corresponding author on reasonable request.

Competing interests

The authors declare that they have no competing interests.

Funding

This research was funded by French National Research Agency (TecItEasy project; ANR-13-AGRO-0007), the French *Institut de Recherche pour le Développement* (IRD) through UMR iEES-Paris, UMR GET and the Pastek program of the GIS-Climat.

Authors' contributions

All authors contributed to the work presented in the manuscript. Olivier Ribolzi and Emma Rochelle-Newall and Oloth Sengtaheuanghoung contributed to the study conception and design. Material preparation and field data collection were performed by Jean-Louis Janeau, Thierry Henri-des-Tureaux, Keooudone Latsachack, Marion Viguier, Christian Valentin and Olivier Ribolzi. Laboratory analysis were conducted by Chanthamousone Thammahacksa, Emilie Jardé, Marion Viguier and Emma Rochelle-Newall. Modelling was performed by Claude Mügler. The first draft of the manuscript was written by Claude Mügler, Olivier Ribolzi and Emma Rochelle-Newall, all authors commented on previous versions of the manuscript. All authors read and approved the final manuscript.

Acknowledgments

The authors would like to thank the Lao Department of Agriculture Land Management (DALAM) and the M-Tropics observatory (Multiscale TROPIcal Catchments; https://mtropics.obs-mip.fr) for their support.

561 **References**

562 Armenise E, Simmons RW, Ahn S, Garbout A, Doerr SH, Mooney SJ, Sturrock CJ, Ritz K
563 (2018) Soil seal development under simulated rainfall: Structural, physical and hydrological
564 dynamics. J Hydrol 556:211-219
565 Assouline S, Mualem Y (1997) Modeling the dynamics of seal formation and its effect on
566 infiltration as related to soil and rainfall characteristics. Water Resour. Res. 33(7):1527-1536
567 Assouline S (2004) Rainfall-induced soil surface sealing: A critical review of observations,
568 conceptual models, and solutions. Vadose Zone J 3(2):570-591
569 Boithias L, Choisy M, Souliyaseng N, Jourdren M, Quet F, Buisson Y, Thammahacksa C,
570 Silvera N, Latsachack KO, Sengtaheuanghoung O, Pierret A, Rochelle-Newall E, Becerra S,
571 Ribolzi O (2016) Hydrological regime and water shortage as drivers of the seasonal incidence
572 of diarrheal diseases in a tropical montane environment. PLoS Negl Trop Dis
573 10(12):e0005195
574 Causse J, Billen G, Garnier J, Henri-des-Tureaux T, Olasa X, Thammahacksa C, Latsachak
575 KO, Soulileuth B, Sengtaheuanghoung O, Rochelle-Newall E, Ribolzi O (2015) Field and
576 modelling studies of Escherichia coli loads in tropical streams of montane agro-ecosystems. J
577 Hydro-environ Res 9:496-507
578 Cho KH, Pachepsky YA, Oliver DM, Muirhead RW, Park Y, Quilliam RS, Shelton DR, 2016.
579 Modeling fate and transport of fecally-derived microorganisms at the watershed scale: State
580 of the science and future opportunities. Water Res 100:38-56
581 Collins R, Elliott S, Adams R (2005) Overland flow delivery of faecal bacteria to a headwater
582 pastoral stream. J Appl Microbiol 99:126-132
583 Gagliardi JV, Karns JS (2000) Leaching of Escherichia coli O157: H7 in diverse soils under
584 various agricultural management practices. Appl Environ Microbiol 66(3):877-883

585 Guber AK, Pachepsky YA, Yakirevich AM, Shelton DR, Sadeghi AM, Goodrich DC,
586 Unkrich CL (2011) Uncertainty in modelling of faecal coliform overland transport associated
587 with manure application in Maryland. Hydrol Process 25(15):2393-2404
588 Guber AK, Shelton DR, Pachepsky YA, Sadeghi AM, Sikora LJ (2006) Rainfall-induced
589 release of fecal coliforms and other manure constituents: Comparison and modeling. Appl and
590 Environ Microbiol 72(12):7531-7539
591 Guber AK, Yakirevich AM, Sadeghi AM, Pachepsky YA, Shelton DR (2009) Uncertainty
592 Evaluation of Coliform Bacteria Removal from Vegetated Filter Strip under Overland Flow
593 Condition. J Environ Qual 38(4):1636-1644
594 Ishii S, Sadowsky MJ (2008) Escherichia coli in the environment: implications for water
595 quality and human health. Microbes Environ 23:101–108
596 Jamieson R, Gordon R, Joy D, Lee H (2004) Assessing microbial pollution of rural surface
597 waters - A review of current watershed scale modeling approaches. Agric Water Manag
598 70(1):1-17
599 Jamieson R, Joy DM, Lee H, Kostaschuk R, Gordon R (2005) Transport and deposition of
600 sediment-associated Escherichia coli in natural streams. Water Res 39(12):2665-2675
601 Janeau JL, Bricquet JP, Planchon O, Valentin C (2003) Soil crusting and infiltration on steep
602 slopes in northern Thailand. European J Soil Sci 54(3), 543-553.
603 Janeau JL, Gillard LC, Grellier S, Jouquet P, Le TPQ, Luu TNM, Ngo QA, Orange D, Pham
604 DR, Tran DT, Tran SH, Trinh AD, Valentin C, Rochelle-Newall E (2014) Soil erosion,
605 dissolved organic carbon and nutrient losses under different land use systems in a small
606 catchment in northern Vietnam. Agri Water Manag 146:314-323
607 Kinnell PI (1993) Runoff as a factor influencing experimentally determined interrill
608 erodibilities. Australian J Soil Sci 31:333-342

609 Kinnell PIA (2005) Raindrop-impact-induced erosion processes and prediction: a review.
610 Hydrol Process 19(14):2815-2844
611 Kollet S, Sulis M, Maxwell RM, Paniconi C, Putti M, Bertoldi G, Coon ET, Cordano E,
612 Endrizzi S, Kikinzon E, Mouche E, Mügler C, Park YJ, Refsgaard JC, Stisen S, Sudicky E
613 (2017) The integrated hydrologic model intercomparison project, IH-MIP2: A second set of
614 benchmark results to diagnose integrated hydrology and feedbacks. Water Resour Res
615 53(1):867-890
616 Kress M, Gifford G (1984) Fecal coliform release from cattle fecal deposits. Water Resour
617 Bull 20(1):61-66
618 Lacombe G, Valentin C, Sounyafong P, de Rouw A, Soulileuth B, Silvera N, Pierret A,
619 Sengtaheuanghoung O, Ribolzi O (2018) Linking crop structure, throughfall, soil surface
620 conditions, runoff and soil detachment: 10 land uses analyzed in Northern Laos. Sci Total
621 Environ 616:1330-1338
622 Le HT, Rochelle-Newall E, Ribolzi O, Janeau JL, Huon S, Latsachack K, Pommier T (2020)
623 Land use strongly influences soil organic carbon and bacterial community export in runoff in
624 tropical uplands. Land Degrad & Dev 31:118-132
625 Luk SH (1979) Effect of soil properties on erosion by wash and splash. Earth Surf Process
626 4:241-255
627 Martinez G, Pachepsky YA, Whelan G, Yakirevich AM, Guber A, Gish TJ (2014) Rainfall-
628 induced fecal indicator organisms transport for manured fields: Model sensitivity analysis.
629 Environ Int 63:121-129
630 Mügler C, Planchon O, Patin J, Weill S, Silvera N, Richard P, Mouche E (2011) Comparison
631 of roughness models to simulate overland flow and tracer transport experiments under
632 simulated rainfall at plot scale. J Hydrol 402(1):25-40

633 Mügler C, Ribolzi O, Janeau JL, Rochelle-Newall E, Latsachach K, Thammahacksa C,
634 Viguier M, Jarde E, Henri-Des-Tureaux T, Sengtaheuanghoung O, Valentin C (2019)
635 Experimental and modelling evidence of short-term effect of raindrop impact on hydraulic
636 conductivity and overland flow intensity. J Hydrol 570:401-410
637 Muirhead RW, Collins RP, Bremer PJ (2006) Interaction of Escherichia coli and soil particles
638 in runoff. Appl and Environ Microbiol 72(5):3406-3411
639 Pachepsky YA, Sadeghi AM, Bradford SA, Shelton DR, Guber AK, Dao T (2006) Transport
640 and fate of manure-borne pathogens: Modeling perspective. Agri Water Manag 86(1-2):81-
641 92.
642 Patin J, Mouche E, Ribolzi O, Sengtahevanghoung O, Latsachak KO, Soulileuth B, Chaplot
643 V, Valentin C (2018) Effect of land use on interrill erosion in a montane catchment of
644 Northern Laos: An analysis based on a pluri-annual runoff and soil loss database. J Hydrol
645 563:480-494.
646 Quansah C (1981) The effect of soil type, slope, rain intensity and their interactions on splash
647 detachment and transport. J Soil Sci 32(2):215-224
648 Ribolzi O, Evrard E, Huon S, Rochelle-Newall E, Henri-des-Tureaux T, Silvera N,
649 Thammahacksac C, Sengtaheuanghoung O (2016) Use of fallout radionuclides (^{7}Be, ^{210}Pb) to
650 estimate resuspension of Escherichia coli from streambed sediments during floods in a
651 tropical montane catchment. Environ Sci Pollut Res 23(4):3427-3435
652 Ribolzi O, Evrard O, Huon S, de Rouw A, Silvera N, Latsachack KO, Soulileuth B, Lefèvre I,
653 Pierret A, Lacombe G, Sengtaheuanghoung O, Valentin C (2017) From shifting cultivation to
654 teak plantation: effect on overland flow and sediment yield in a montane tropical catchment.
655 Scientific Reports 7(1):3987

656 Ribolzi O, Patin J, Bresson LM, Latsachack KO, Mouche E, Sengtaheuanghoung O, Silvera
657 N, Thiebaux JP, Valentin C (2011) Impact of slope gradient on soil surface features and
658 infiltration on steep slopes in northern Laos. Geomorphology 127(1-2):53-63
659 Rochelle-Newall E, Nguyen TMH, Le TPQ, Sengteheuanghoung O, Ribolzi O (2015) A short
660 review of fecal indicator bacteria in tropical aquatic ecosystems: knowledge gaps and future
661 directions. Front Microbiol 6:308
662 Rochelle-Newall E, Ribolzi O, Viguier M, Thammahacksa C, Silvera N, Latsachack KO,
663 Rinh PD, Naporn P, Hai Tran S, Soulileuth B, Hmaimum N, Sisouvanh P, Robain H, Janeau
664 JL, Valentin C, Boithias L, Pierret A (2016) Effect of land use and hydrological processes on
665 Escherichia coli concentrations in streams of tropical, humid headwater catchments. Scientific
666 Reports 6:32974
667 Rosebury T (1962) Microorganisms indigenous to man. New York: McGraw-Hill Co
668 Silburn DM, Connolly RD (1995) Distributed parameter hydrology model (ANSWERS)
669 applied to a range of catchment scales using rainfall simulator data I: Infiltration modelling
670 and parameter measurement. J Hydrol 172(1):87-104
671 Tatard L, Planchon O, Wainwright J, Nord G, Favis-Mortlock D, Silvera N, Ribolzi O,
672 Esteves M, Huang CH (2008) Measurement and modelling of high-resolution flow-velocity
673 data under simulated rainfall on a low-slope sandy soil. J Hydrol 348(1-2):1-12
674 Unc A, Goss MJ (2004) Transport of bacteria from manure and protection of water resources.
675 Appl Soil Ecol 25(1):1-18
676 Valentin C, Agus F, Alamban R, Boosaner A, Bricquet JP, Chaplot V, de Guzman T, de
677 Rouw A, Janeau JL, Orange D, Phachomphonh K, Phai Do Duy, Podwojewski P, Ribolzi O,
678 Silvera N, Subagyono K, Thiébaux J, Toan T, Vadari T (2008) Runoff and sediment losses
679 from 27 upland catchments in Southeast Asia: Impact of rapid land use changes and
680 conservation practices. Agric Ecosyst Environ 128:225-238

Wei W, Chen L, Fu B, Huang Z, Wu D, Gui L (2007) The effect of land uses and rainfall regimes on runoff and soil erosion in the semi-arid loess hilly area, China. J Hydrol 335(3-4):247-258

Weill S, Mouche E, Patin J (2009) A generalized Richards equation for surface/subsurface flow modelling. J Hydrol 366(1):9-20

Wilkinson J, Jenkins A, Wyer M, Kay D (1995) Modeling fecal-coliform dynamics in streams and rivers. Water Res 29(3):847-855

Woolhiser DA, Smith RE, Goodrich DC (1990) KINEROS, a kinematic runoff and erosion model: Documentation and user manual. U.S Department of Agriculture, Agricultural Research Service, ARS-77, 130pp

World Health Organisation (2014) Progress on Drinking Water and Sanitation, WHO Library Cataloguing-in-Publication Data, Avenue Appia, 1211 Geneva 27, Switzerland

Ziegler AD, Sutherland RA, Giambelluca TW (2000) Partitioning total erosion on unpaved roads into splash and hydraulic components: The roles of interstorm surface preparation and dynamic erodibility. Water Resour Res 36(9):2787-2791

Figure captions:

Fig. 1

Study site: **(a)** Aerial view of the Houay Pano catchment (white dotted polygon) and location of the experimental site (white rhombus); **(b)** Picture showing an overview of the hillslope and the experimental site with the rainfall simulator tent on the right

Fig. 2

Experimental design: **(a)** image of one 1-m^2 metallic frame divided into two sub-plots without mosquito net (left) and with mosquito net (right); **(b)** Diagram showing the nine plots (pairs of 9 sub-plots without mosquito net shown in white, associated with 9 sub-plots covered with mosquito net shown in colour) divided in triplicated treatment groups (A, B, C): controls with no amendments (Ref A, Ref B, and Ref C) or amended with pig manure (Pig A, Pig B, and Pig C) or poultry manure (Chi A, Chi B, and Chi C); **(c)** Image of one sub-plot partially covered with disconnected small patches of chicken manure ; **(d)** Chronological sequence for the three rainfall simulations (R1, R2 and R3) and time of amendment with pig or chicken manure

Fig. 3

Bar plots showing cumulated **(a)** runoff depth and **(b)** soil erosion from the eighteen 0.5m^2 sub-plots (i.e. nine without plus nine with mosquito net) divided into triplicated treatment groups (A, B, C). Controls with no amendments (Ref) or amended with pig manure (Pig) or poultry manure (Chi). Measurements were conducted during the first rainfall simulation (R1, before manure application) and the second rainfall simulation (R2, after manure application)

Fig. 4

E. coli concentration in runoff water from both sub-plots without mosquito net (left side, with splash effect) and with mosquito net (right side, with limited splash effect) for the triplicated plots Ref, Pig, and Chi for rainfall simulation R2

Fig. 5

Evolution over time on plot Chi A of the runoff coefficient (Runoff/Rainfall) obtained during R2 **(a)** and R3 **(b)**; the sediment outputs obtained during R2 **(c)** and R3 **(d)**; *E. coli* concentrations obtained during R2 **(e)** and R3 **(f).** In each figure, empty and filled symbols correspond to the experimental results for the sub-plots with and without a mosquito net, respectively. Solid lines correspond to the modelled evolutions with mosquito net (grey) and without mosquito net (black)